Disclination Core Structure in Rigid and Semiflexible Main-Chain Polymer Nematic Liquid Crystals

Steven D. Hudson*

Department of Polymer Science & Engineering, University of Massachusetts, Amherst, Massachusetts 01003

James W. Fleming, Eugene Gholz, and Edwin L. Thomas

Department of Materials Science & Engineering, Massachusetts Institute of Technology, Cambridge, Massachusetts 02139

Received July 27, 1992; Revised Manuscript Received November 24, 1992

ABSTRACT: In order to ascertain the near-core structure of $\pm^1/_2$ wedge disclinations, the apparent splay and bend elastic anisotropy, ϵ_{app}, is measured as a function of radial distance from the singularity. $\epsilon_{app} = [(k_{11})_a - (k_{33})_a]/[(k_{11})_a + (k_{33})_a]$. Both a rigid and a semiflexible main-chain liquid crystal polyester are studied. Results demonstrate a special structure of the core at radii less than about several molecular lengths. The rigid material splays significantly more; at a distance of 0.1 μm, ϵ_{app} is approximately −0.4, yet the asymptotic value, ϵ (at a distance of 1 μm), is approximately 0. In contrast, the semiflexible material bends more; ϵ_{app} (0.1 μm) $\sim$ 0.1 and $\epsilon \sim -0.15$. These results can be understood in terms of the molecular lengths and relative rigidities of these liquid crystalline materials. The presence of hairpins in the flexible-chain polymer is suggested.

Introduction

Disclination defects in liquid crystals show a wide variety of topological structures.[1] They also appear to dominate rheological behavior at some deformation rates.[2] Related to both of these issues is the structure of the disclination core region. Unfortunately, however, the structure of the core is little known. Even theoretical work is not well advanced. Disclinations of strength ±1 in uniaxial materials are free to escape into the third dimension and therefore have a nonsingular core as described by Meyer[3] and Cladis and Kleman.[4]

The $\pm^1/_2$ disclinations, however, cannot escape—unless the material undergoes a phase transition. The unescaped structure has a singularity at the core. The material will distort in some way to avoid this singularity, but the mode of distortion is not obvious. Biaxial nematics may avoid a singularity in the weak directors by escaping to a uniaxial core.[5] This phase change may be second order, resulting in a diffuse boundary between the phases. For uniaxial nematics, the situation is less clear. Ericksen proposed that, approaching the singularity, the material would experience a first-order transition to an isotropic core.[6] The interface between nematic and isotropic would be sharp, and the core region is predicted to be a molecular size. Outside the core region the structure may be effected by a number of factors unconsidered by Ericksen: surface tension, director anchoring energies, and elastic anisotropy.[5] The elastic constants in the highly strained core may have values different from those in the bulk since the order parameter may vary.

Schopohl and Sluckin have calculated the structure of $\pm^1/_2$ disclinations within the Landau–de Gennes framework.[7] They find that the material near the core continuously changes from uniaxial to biaxial, with maximum biaxial character at some distance from the center of the core. The radius of maximum biaxiality may change with temperature.

To date, the most informative experimental results on disclination core structure are those of Mazelet and Kleman,[8] who studied a polymeric system where the splay–bend elastic anisotropy is nearly 1. From optical microscopy, Mazelet and Kleman conclude that the $^1/_2$ disclination core is larger and scatters light much more strongly than that of the $-^1/_2$ disclination. They suggest a large concentration of chain ends at the $^1/_2$ disclination core, with director alignment parallel to the core axis for the $-^1/_2$ disclination. An aggregation of chain ends at the $^1/_2$ disclination core would introduce splay distortion and decrease k_{11}. This increase in the splay distortion would reduce the apparent elastic anisotropy near the core.

A core of different apparent elastic anisotropy in small-molecule liquid crystals (SMLC) (if it were possible) might not greatly influence the mobility of a disclination. In polymer liquid crystals, however, such a concentration of chain ends would make disclination motion nonconservative and significantly decrease their mobility. Cladis has observed the dynamics of $-^1/_2$ disclinations in small molecules.[9] The disclination core drags surrounding material with it as it moves, in order to reduce director rotations. In liquid crystalline polymers (LCPs), a concentration of chain ends at a disclination core may enhance this behavior. Mazelet and Kleman observed higher mobility for the $-^1/_2$ than for the $^1/_2$ disclination.[8]

In light of these studies which predict inhomogeneous structure at the near-core region of a disclination, we investigate the *apparent* splay and bend Frank elastic constant anisotropy as a function of radial distance from the disclination. The elastic anisotropy is defined as

$$\epsilon = \frac{k_{11} - k_{33}}{k_{11} + k_{33}} \tag{1}$$

where k_{11} is the splay and k_{33} is the bend elastic constant. The apparent elastic anisotropy, ϵ_{app}, is given by

$$\epsilon_{app}(r) = \frac{k_{11_a}(r) - k_{33_a}(r)}{k_{11_a}(r) + k_{33_a}(r)} \tag{2}$$

where $k_{11_a}(r)$ and $k_{33_a}(r)$ are now functions of distance from the core singularity.

The present work concerns the static structure of the core region, using the TEM director imaging technique developed by Thomas and Wood.[10] The director is revealed in the TEM images by crystalline lamellae 15 nm thick. Therefore, we are able to probe the radial structure of the director field from approximately the scale of a few lamellae (0.1 μm) to a fraction of the separation between

0024-9297/93/2226-1270$04.00/0

disclinations (a few microns). Because this lamellar decoration technique has superior resolution of the director, it is expected to be excellent in observing perturbations from the far-field director pattern about a disclination as one nears the disclination core. However, it cannot measure changes in the local order parameter, which are expected in the very center of the disclination (<0.1 μm). Although the "inner" disclination core structure remains an elusive goal, the lamellar decoration technique reveals the most detailed information to date regarding the structure of the "outer" disclination core.

Frank elastic theory applies where the distortions in the director field are weak compared to molecular dimensions. Therefore, far from the disclination, where the distortions are weak, the elastic anisotropy, ϵ, can be calculated from the structure of the disclination.[11] In this paper, we observe, for the first time, the structure of the disclination within a few molecular lengths of its center. In this case, the distortions exceed that which can be described by Frank elastic theory.

Two different consequences of the increased distortion may be envisioned. First, nonlinear corrections to the Frank elastic theory become important when the distortion becomes large compared to the molecular size. These corrections lead to an apparent rise in the splay constant when the splay distortion approaches $1/L$, where L is the molecular length. Similarly, they lead to an apparent rise in the bend constant when the bend distortion approaches $1/p$, where p is the persistence length. These corrections can be calculated for lyotropic LCPs, but, unfortunately, no theory is yet able to predict them in thermotropics. Second, because these materials are polydisperse, the distortion may promote segregation of different species at the core leading to *real* changes in the elastic constants. Regardless of the ambiguity as to whether the apparent change in ϵ is due to inapplicability of the theory or due to real changes in material composition, we are able to measure real structural variation. The relative amounts of splay and bend are different near the core from that found asymptotically far from the disclination. To describe this structural variation, it is useful to calculate an apparent elastic anisotropy, ϵ_{app}, in order to measure the relative splay and bend distortions as a function of radial distance from the disclination center.

Method

We study two different polymers. The first is a semiflexible polymer[12] which we term TQT10-H:

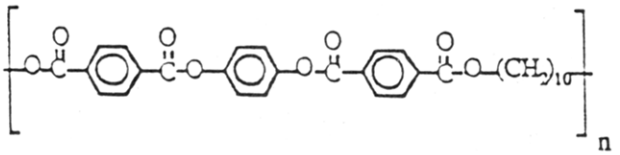

This polymer has its glass transition at 67 °C and becomes nematic at 231 °C and isotropic at 267 °C. The molecular weight is estimated to be ~18 000 from intrinsic viscosity measurements. The length, L, for the fully extended polymer is approximately 100 nm. If many folds (hairpins) are present, the effective, L_{eff}, is significantly reduced.

The other polymer, QT-OEOM, is more rigid:[13]

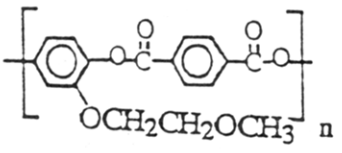

This polymer has its glass transition at 120 °C and becomes nematic at 180 °C and isotropic at 224 °C. Estimates of the persistence length in dilute solution vary from 10 to 79 nm.[14,15] In either case, tight folds or hairpins are impossible. Estimating the molecular weight to be 5000, L is 24 nm, or approximately the persistence length.

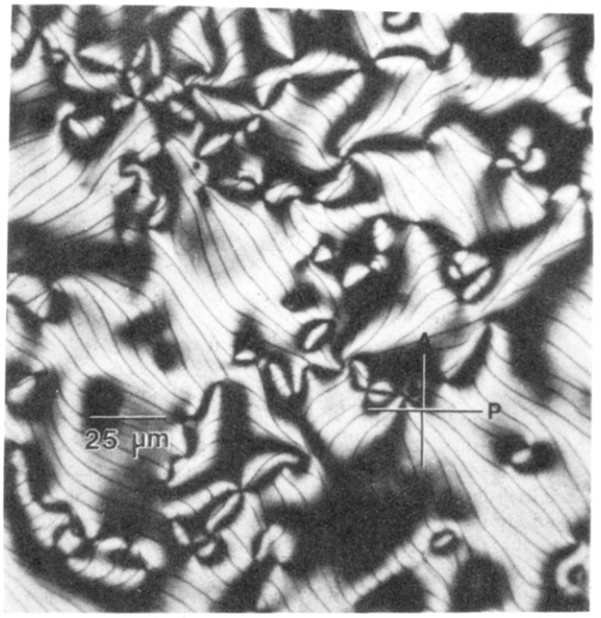

Figure 1. Optical micrograph of a QT-OEOM thin film in the glassy state. Polarizer and analyzer directions are indicated. A schlieren texture is frozen in. The thin dark filaments shown are hairline cracks which formed when the polymer was quenched to room temperature. These cracks are parallel to the director.

To measure the apparent elastic anisotropy as a function of distance from a disclination, we would ideally examine isolated disclinations. Disclination interaction is a very important effect which can dominate the results. For a $^1/_2$ disclination, the measured value of ϵ_{app} (assuming weak anisotropy) differs from the true value by

$$\Delta\epsilon_{app} \approx 2r/3d \tag{3}$$

where r is the radius at which the apparent elastic anisotropy is measured and d is the distance to the neighboring disclination. (This equation will be derived in the Results and Discussion section.) If we want to limit the effect of disclination interaction to $\Delta\epsilon_{app} \approx \pm 0.1$, we require disclination separations greater than 7 μm. The effects of many neighboring disclinations may or may not offset.

This requirement for disclination separation is difficult to achieve in typical thermotropic liquid crystal polymers (TLCPs). The technique of surface tension spreading described in an earlier paper works well sometimes.[11] The TQT10-H sample was spread at a temperature of 240 °C. This technique lacks reproducibility, however, as director distortions are sometimes introduced during the flow.

A more reproducible method of obtaining a schlieren texture of disclinations each separated by several microns has been developed which works especially well for the rigid material. Polymer, placed between a glass slide and a coverslip, is melted on a hotplate to form a film approximately 1 μm thick. The film is thin enough to ensure a planar texture. The coverslip is oscillatory sheared by hand with a slow rate and small amplitude. A coarse schlieren texture results. The sample is cooled to liquid-nitrogen temperatures, and the two slides are cleaved apart. The sample is heated again to the mesophase to allow the fracture surface to smooth itself. Finally, the sample is quenched in room-temperature water. The resulting polymer is glassy with few crystals. The QT-OEOM sample presented here was held near 200 °C for a few minutes before quenching.

Figure 1 shows a glassy schlieren texture of QT-OEOM. The molecular orientation lies in the film plane, and where it is parallel to either the polarizer or analyzer, the image appears dark. Disclinations are found where the dark regions are narrowest. These defect lines are normal to the film and are typically several

microns apart. Both integer and half-integer defects are present. Spiral cracks highlight an $s = 1$ disclination in the upper part of the figure. These cracks along the molecular director result from shrinkage of this especially brittle polymer during quenching. Although these cracks present an interesting decoration method of their own, their presence raises the concern of polymer shrinkage upon quench. However, shrinkage is not expected to cloud the results of this work. Isotropic shrinkage has no effect on the measured values of ϵ_{app}. Anisotropic shrinkage (different shrinkage parallel and perpendicular to the chain) slightly changes the value of ϵ_{app}, but the change in ϵ_{app} is independent of r.

Controlled growth of small lamellar crystals is used to decorate the director field to permit direct observation via the TEM.[10] A glassy nematic thin film TLCP sample may be annealed at approximately 20 °C below the melting point for approximately 30 min. During annealing, the quenched nematic polymer partially crystallizes in a lamellar morphology, where the director of the remaining glassy liquid crystal is normal to the lamellae. When viewed in TEM, lamellae are seen edge-on and appear dark. The lamellae serve to decorate the underlying molecular arrangement of the frozen nematic, revealing a 30-nm resolution map of the director field (see Figure 2). To get effective decoration, the crystals should be smaller than the size of the distortions. When this condition is met, the director is observed to vary smoothly with position. Primary nucleation density of crystals must be large, while crystal growth is relatively slow.

Phase contrast is principally responsible for imaging the lamellae. At zero defocus the lamellae are hardly visible. Because the lamellar repeat is approximately 30 nm, a large amount of defocus (~−10 μm) is desired to properly image this periodicity. Near-zero defocus is useful for imaging the size and shape of crystals by diffraction contrast. Typical crystal sizes are 15 (thick) × 80 × 80 nm.

Thomas and Wood's lamellar decoration technique requires thin films for observation of TEM, so the oscillatory shear sample preparation technique described above, requiring films at least 1 μm thick, is not directly useful. We have, however, developed an etch technique which extends the usefulness of the lamellar decoration technique to thick samples.[16] The TLCP sample is again prepared in the mesophase, quenched, and annealed. The polymer surface is then etched in a methylamine solution which preferentially removes the noncrystalline material between lamellae. The resulting surface profile with protruding lamellae is replicated by standard techniques. Pt is shadowed at a 30° angle, and a carbon support film is evaporated normal to the surface. Figure 2 shows a replica image of a positive $^1/_2$ wedge disclination present in the QT-OEOM sample. The hairline cracks, seen in Figure 1, appear as the large dark features in Figure 2. There is inevitable loss of detail in the upper right of this figure where the lamellae are parallel to the shadowing direction. This loss of detail presents a complication.

The core structure which has been measured in this work may also be qualitatively seen by eye. To demonstrate, Figure 3 shows sketches and images of disclinations having either more bend or more splay at the core.

To facilitate unbiased data collection of the director field $\mathbf{n}(\mathbf{r})$, a digital image processing algorithm has been developed. Disclination images are digitized using a video camera, with only the center of the images used in order to avoid peripheral image distortions introduced by the camera. Small local images are extracted from all areas of each digitized image. These local images are filtered though a Hamming window, commonly used in signal processing to eliminate artificial oscillations produced by filtering.[17] The Hamming window has the following transmission as a function of radius:

$$T = 0.54 + 0.46\cos(2\pi R/D), \quad \text{for } R < D/2$$

$$T = 0, \quad \text{for } R > D/2 \tag{4}$$

where D is the size of the local image. The local image is Fourier transformed, and the director orientation is determined from the angular position of the peak in the resulting power spectrum.

Although the lamellae in an image such as in Figure 2 are clearly seen by eye, there is sufficient noise where the lamellae are parallel to the shadowing direction that the local power spectrum does not contain a strong peak corresponding to the director. The image can be accurately and reproducibly traced with a pen, and the resultant tracing can be digitized and processed. Figure 4 shows the superposition of a trace and the map of local normals to the director field calculated from the trace. The calculated director field accurately reproduces the trace. The radius of the Hamming window, as characterized by the radius at half-maximum transmission, used in processing this image is 77 nm.

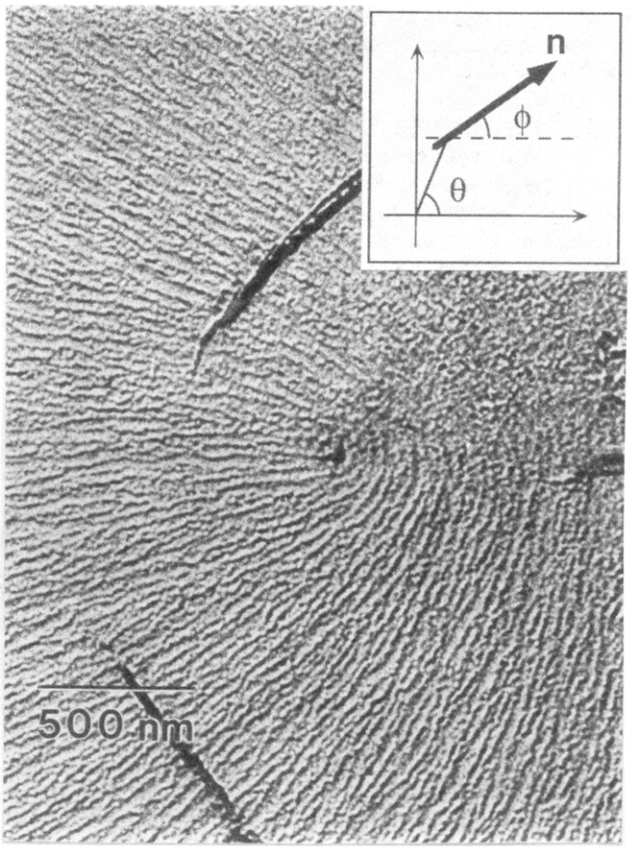

Figure 2. TEM micrograph of a replica of the QT-OEOM film shown in Figure 1 showing the core region of $^1/_2$ disclination. The large dark features are the cracks observed in Figure 1. The striations are due to the lamellar crystals. The director is normal to the lamellae.

The images of the flexible polymer, TQT10-H, are of thin films which were not replicated. They do not suffer the problem due to shadowing, so both traces and the images themselves were processed to calculate the director field. The window radius used in processing was 67 nm.

Analysis

Output from the processing program is the director angle, ϕ ($\mathbf{n} = \cos\phi, \sin\phi$), at data points corresponding to the location of the center of each window. The position of the disclination can easily be measured from the superposition of the image (or trace) and the director field. To measure the elastic anisotropy as a function of the distance from the disclination, $\phi(r,\theta)$ data are desired where θ is the azimuthal angle $(0, 2\pi)$ about the disclination (see the inset in Figure 2). All data points inside the shell between r and $r + \Delta r$ are included in $\phi(r,\theta)$. The number of data points increases with the radius. Figure 5 shows $\phi(r,\theta)$ data obtained from Figure 2; here, $\Delta r = 39$ nm.

The apparent elastic anisotropy, ϵ_{app}, is determined by the least-squares fit of the data, $\phi(r,\theta)$, to the first-order perturbation expansion in terms of ϵ_{app}.[18,19]

$$\phi_{calc}(\theta) = s\theta_0 + s\theta - \epsilon_{app}s(2-s)/(4(1-s)^2)\sin(2(1-s)(\theta-\theta_0)) \tag{5}$$

where s is the disclination strength and θ_0 is the orientation

of the disclination. Because the perturbation is a sine function, ϵ_{app} may be calculated from the Fourier coefficients of the perturbation part of the data ($\phi(r,\theta) - s\theta$). These Fourier coefficients are known to give a least-squares fit to the data.[20] Because ϕ_{calc} is independent of r, each radius is treated independently. Only the pertinent Fourier coefficients are calculated: a_0, a_i, and b_i, where $i = 2(1 - s)$. (a_i is the ith cosine coefficient.)

θ_0 and ϵ_{app} are calculated from the coefficients as follows:

$$\theta_0 = a_0/(2s) \tag{6a}$$

$$\epsilon_{app} = -4(1-s)^2/(s(2-s))(a_i^2 + b_i^2)^{1/2} \cos \alpha \tag{6b}$$

$$\alpha = 2a_0(1 - s) - \tan^{-1}(a_i/b_i) \tag{6c}$$

α is a measure of the phase shift between the ith Fourier coefficients and determines the sign of ϵ_{app}. For an isolated symmetric disclination, α is an integer multiple of π.

If the director field is distorted, a_i and b_i may both include a contribution from the distortion. If the type of distortion is known, then the effects of the distortion may be subtracted from the coefficients. We discuss distortions due to neighboring disclination interactions later.

If there is noise in the data, only the contribution due to the noise which is in-phase with the orientation of the disclination alters the results. The effect of noise is to increase the error bars in the calculation of ϵ_{app}.

Figure 5 shows $\phi(r,\theta)$ data from the disclination depicted in Figure 2 at $r = 0.12$ and 1.01 μm from the singularity and the calculated fitting function, ϕ_{calc}, in each case. The root sum square errors, $[\sum(\phi_{calc}(\theta_i) - \phi(\theta_i))^2]^{1/2}$, are 0.445 and 0.633 rad, respectively.

Results and Discussion

Most of our measurements of the apparent elastic anisotropy are of $^1/_2$ disclinations. We will present these data first and then follow with preliminary data from $^{-1}/_2$ disclinations. Parts a and b of Figure 6 show $\epsilon_{app}(r)$ for positive $^1/_2$ disclinations of QT-OEOM and for TQT10-H. Figure 6c shows the respective data in parts a and b of Figure 6 averaged.

Results demonstrate that $\epsilon_{app}(r)$ levels off at radii greater than about 0.5 μm for both polymers. For the more rigid polymer, at a distance of 0.1 μm, ϵ_{app} is approximately −0.4, yet the asymptotic value, ϵ (at a distance of 1 μm), is approximately 0. In contrast, the flexible material bends more at the core; ϵ_{app} (0.1 μm) $\approx$ 0.1 and $\epsilon \approx -0.15$.

These results follow the trend expected for changes in the apparent elastic constants due to nonlinear corrections to Frank theory. Splay requires entropically disfavored aggregation of chain ends (or hairpins, if they are possible), and the Frank splay elastic constant is proportional to the effective molecular length, L.[21] Nonlinear corrections to the splay constant become significant when the amount of splay approaches $1/L$. Similarly, corrections to the bend constant occur when the amount of bend approaches $1/p$, where p is the persistence length. The flexibility of the chain determines which correlation is dominant. If $p \ll L$, the apparent splay constant increases significantly, while corrections to the bend constant are negligible. If p is at least L, however, corrections to the bend constant may be larger than those to the splay constant.[22]

Approaching a disclination, both bend and splay distortions tend to grow as $1/r$. Therefore, at radii less than a few L, flexible polymers ($p \ll L$) bend more in order to reduce the aggregation of chain ends or hairpins. The bend elastic constant is independent of radius, while the splay constant apparently increases. Therefore, ϵ_{app} will increase near the disclination. If, however, the polymer is stiff, the entropy penalty of aggregating chain ends is

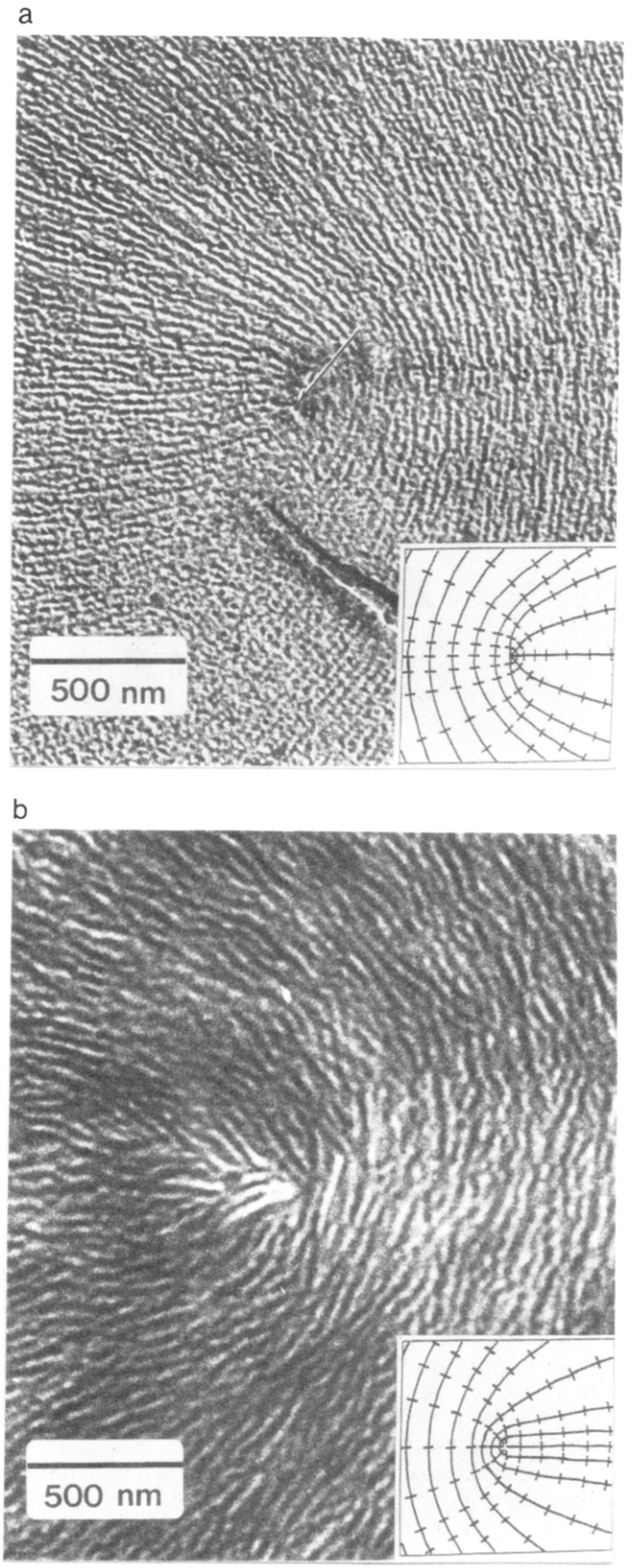

Figure 3. (a) A $^1/_2$ disclination of the rigid polymer which has more splay at the core. Because the lamellae are perpendicular to the director, the lamellae appear to bend more at the core (see also Figure 2). The disclination center is marked with an arrow. The inset is a sketch of a disclination having more splay at the core. The director field is shown as the solid lines, while the lamellae, which are perpendicular to the director, are drawn as hash marks. (b) A $^1/_2$ disclination of the flexible material which has more molecular bend at the core. The lamellae appear to splay more. The inset is a sketch of a disclination having more bend at the core.

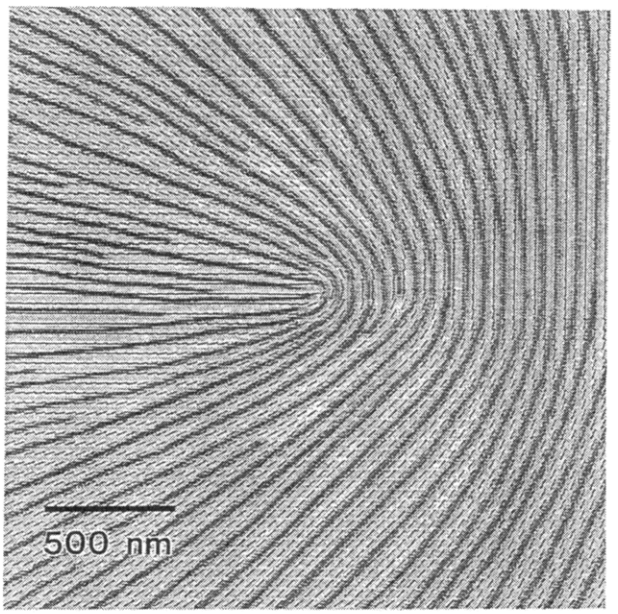

Figure 4. Results of the image processing (shown as hash marks) overlaid on a trace of Figure 2. Both the trace and the hash marks are perpendicular to the calculated director.

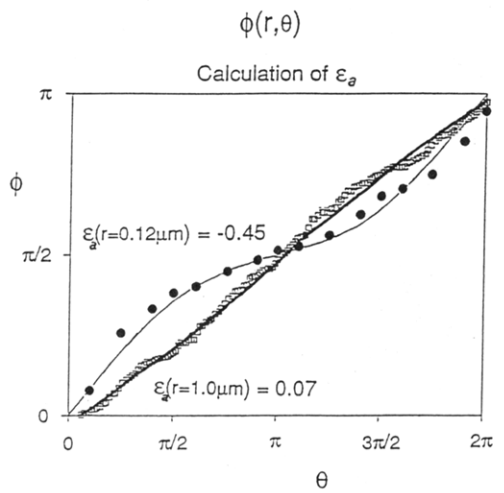

Figure 5. Data taken from Figure 4 at two different radii. The curves which fit the data are generated from the Fourier coefficients calculated from the data as described in the text. ϵ_{app} at 0.12 μm is −0.45; ϵ_{app} at 1.0 μm is 0.07.

considerably less than the energetic cost of molecular bending, so that the apparent bend constant increases more rapidly toward the disclination center than the splay constant. Consequently, ϵ_{app} decreases at the core. These trends precisely are observed in Figure 6.

The radial extent of this outer core region may be indicative of the molecular lengths. In the rigid material, deviations from the asymptotic value of ϵ become discernible at radii of approximately $20L$ (~400 nm). In the flexible material, one expects deviations to be discernible at a greater distance from the core, due to the considerably larger contour length for the THT-10 polymer. The data, however, indicate approach to the asymptotic value of ϵ at a relatively short distance (500 nm) from the core. This suggests that the flexible chain reduces its effective length through the introduction of hairpins. Since the average effective chain length for n hairpins varies as L/n, in order to reduce the effective chain length to approximately 20 nm an average of one out of every eight flexible spacers could be folded. Hairpins in the flexible-chain polymer are therefore expected to be semidilute. The concentration of hairpins does not dramatically increase toward the disclination center since ϵ_{app} increases there.

Not only the trend of $\epsilon_{app}(r)$ but also the asymptotic value, ϵ, is indicative of the molecular structure. For both polymers, ϵ is nearly 0 even though the stiffness of the molecular backbones are very different. These polymers behave neither as flexible molecules of infinite length (ϵ approaching 1) nor as finite length and perfectly rigid rods (ϵ approaching −1). Increased stiffness of a molecule tends to decrease ϵ, while increased molecular length tends to increase ϵ. Because ϵ for the rigid, shorter chain material is slightly greater than for the flexible, longer chain, some chain end coupling may exist in the rigid material.[21] Chain end coupling increases the effective molecular length and may be enhanced by hydrogen bonding of acid end groups.[8] However, the existence of chain end coupling or hairpins cannot be proven without further detailed observations of $\epsilon_{app}(r)$ as a function of molecular weight.

Impurities and polydispersity of molecular weight may also be important. To increase the concentration of chain ends near the core, lower molecular weight material may be segregated. The increased concentration of chain ends near half integer disclinations in rigid polymers may retard their mobility.

While the $^1/_2$ disclination simply acts as a source of high distortion, $^{-1}/_2$ disclinations impose an additional geometric constraint, due to the nature of splay in these defects. Splay in $^1/_2$ disclinations (positive splay) causes director field lines to *converge* upon the core. On the other hand, (negative) splay in $^{-1}/_2$ disclinations causes field lines to *diverge* from the core. Results of $\epsilon_{app}(r)$ for $^{-1}/_2$ disclinations in the rigid polymer are shown in Figure 7. The asymptotic value of the elastic anisotropy approaches that for the $^1/_2$ disclinations only at radii of about 1 μm. Contrary to the positive defects, $\epsilon_{app}(r)$ increases steadily on approaching the core before rapidly turning over to negative values at very small (~0.1 μm) distances. This behavior may be understood as due to the geometrical difference of the director field in the two types of defect. In the case of a positive disclination, an arbitrary amount of (positive) splay can be accommodated at the disclination center, whereas for a negative disclination, large amounts of (negative) splay are inhibited because the flux of director lines is toward the region of greater splay, which requires ever more chain ends (or hairpins). Negative splay is incompatible with long molecules, where chain ends are dilute. Since splay will be avoided at a $^{-1}/_2$ core, rigid materials are thus expected to bend more than at a $^1/_2$ core. The slightly positive value of $\epsilon_{app}(r)$ in Figure 7 is consistent with this scenario. Finally approaching the inner core region of the $^{-1}/_2$ defect, $\epsilon_{app}(r)$ is observed to decrease sharply. This is similar to the inner core region behavior of the rigid materials for $^1/_2$ defects. This inner core behavior may result from segregation of the lowest MW molecules. In order to maintain constant material density at the $^{-1}/_2$ core, splay requires a shorter effective chain length. This may be accommodated in flexible chains by hairpin folding. Since folding is prohibited for rigid chains, the amount of bend must increase. We were not able to investigate the $^{-1}/_2$ defects in the semiflexible material.

Turning now to a discussion of possible sources of error and limitations to our approach, we first discuss the fitting function used to find ϵ. The fitting function is a perturbation function valid only when ϵ is small. How good is this approximation? It works to our advantage that $|\epsilon|$ never gets very big: $-1 < \epsilon < 1$. The quality of the fit also depends on the strength of the disclination and the number of data points. The effect of the number of data points, however, is not significant, since low-frequency coefficients are being calculated. For a $^1/_2$ disclination and infinitely many data points, the calculated value of ϵ is 0.85 when

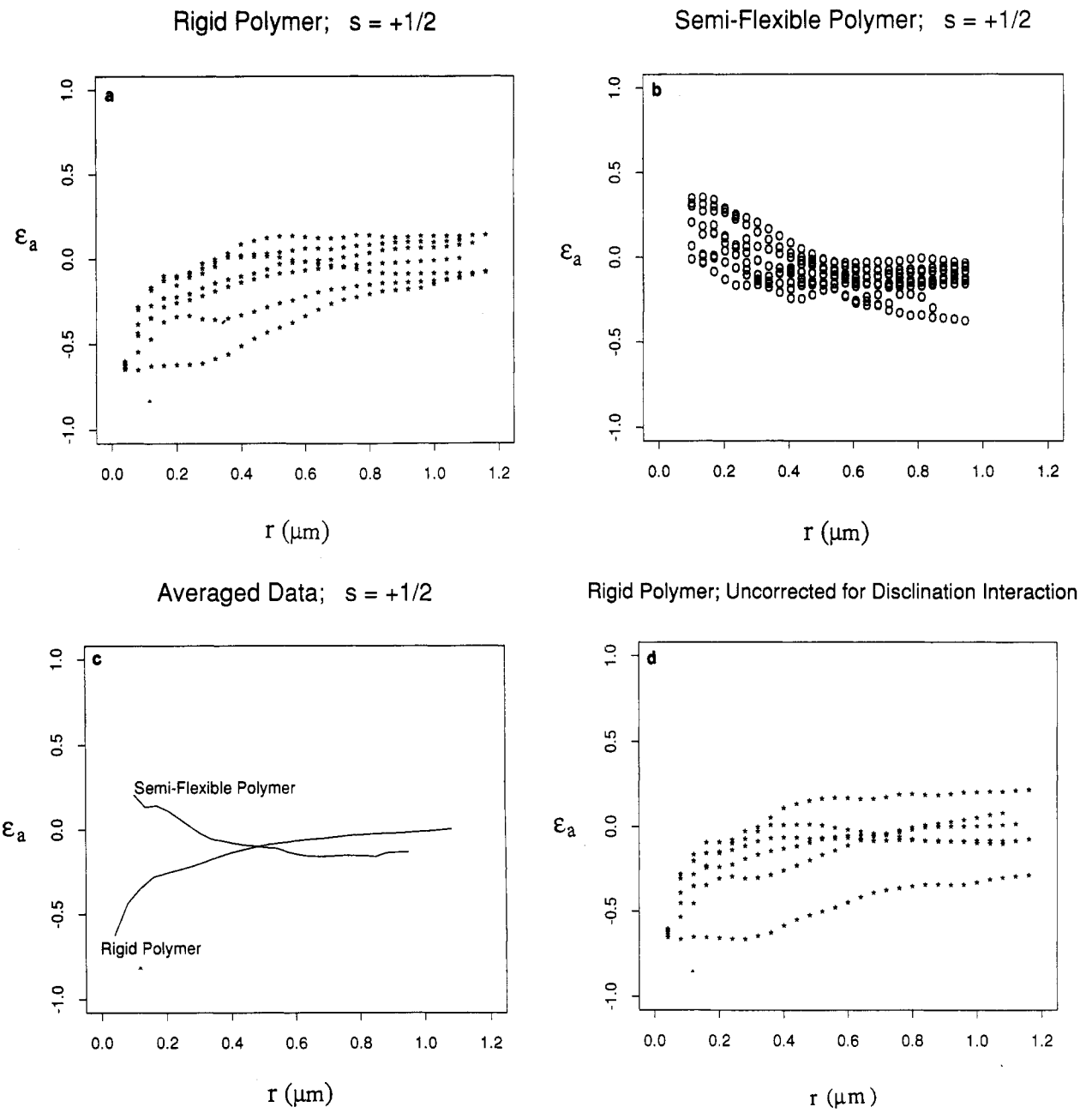

Figure 6. $\epsilon_{app}(r)$ results for $^1/_2$ disclinations in (a) QT-OEOM, (b) TQTQ10-H, and (c) average curves for both polymers. ϵ_{app} positive indicates excess bend distortion; ϵ_{app} negative indicates excess splay distortion. (d) $\epsilon_{app}(r)$ results as in Figure 6, but without correction for disclination interaction.

$\epsilon = 1$ and 0.48 when $\epsilon = 0.5$. Near the core, there are fewer data points to calculate the coefficients: at the disclination core the number of the data points may be as few as eight. When only eight data points are used, ϵ is calculated to be 0.89 when $\epsilon = 1$. Even for the extreme values of ϵ, the fitting function is off by at most 15%. For typical values of ϵ and for $\pm^1/_2$ disclinations, the fitting function is accurate to better than 5%. The trends observed in parts a and b of Figure 6 are not significantly affected by our choice of a simple fitting function.

On the other hand, the effect of disclination interaction can be quite significant. In the limit of small elastic anisotropy, the effect of a neighboring disclination on $\phi(\theta)$ may be added to eq 5 (which is for an isolated disclination)[19]

$$\phi(\theta) = s\theta_0 + s\theta - \epsilon s(2-s)/(4(1-s)^2)\sin(2(1-s)(\theta-\theta_0)) + s_d \tan^{-1}((y - d\sin\theta_d)/(x - d\cos\theta_d)) \quad (7)$$

where (d, θ_d) locates the position of the neighboring disclination with strength s_d. To find the effect of the neighbor on the calculated value of ϵ, simply calculate the appropriate Fourier term of the last term in eq 7. For a $^1/_2$ disclination interacting with one neighbor, the director field is approximately

$$\phi(\theta) = \theta_0/2 + \theta/2 - \epsilon(3/4)\sin(\theta - \theta_0) + s_d(\theta_d - \pi) - s_d(r/d)\sin(\theta - \theta_d) \quad (8)$$

The apparent change in the observed ϵ is

$$\Delta\epsilon_{app} = (s_d/3)(r/d)\cos(\theta_d - \theta_0) \quad (9)$$

This can be subtracted from the calculated value of ϵ to get a corrected value. Figure 6a showed data corrected for disclination interaction in this way. Figure 6d shows the uncorrected data from QT-OEOM. A variety of orientations and distances for the neighboring disclinations are represented. This simple correction accounts for some of the spread in the data. Nonlinear effects of disclination interaction cannot be evaluated at the present time. For $-^1/_2$ disclinations, the effect of neighboring disclinations is limited because the 3-fold symmetric Fourier component is small.

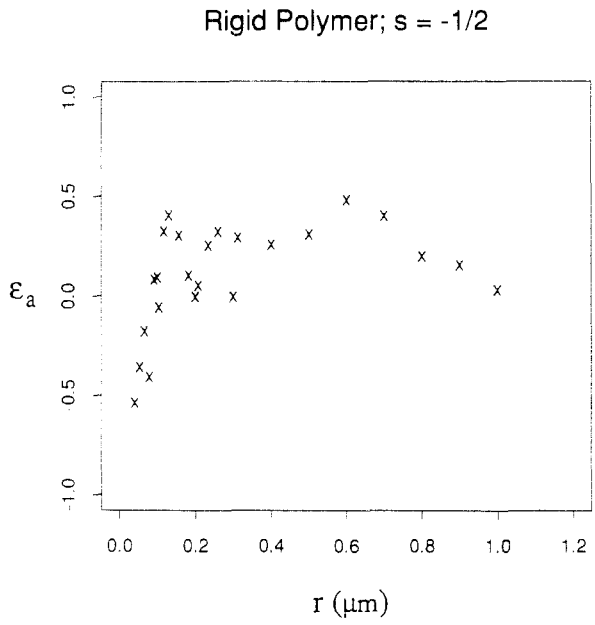

Figure 7. $\epsilon_{app}(r)$ results for $-1/2$ disclinations in QT-OEOM.

A similar analysis can be made of the effect of miscentering the origin on the disclination:

$$\phi(\theta) = s\tan^{-1}((y - \Delta r\sin\theta_d)/(x - \Delta r\cos\theta_d)) - \epsilon s(2-s)/(4(1-s)^2)\sin(2(1-s)(\theta-\theta_0)) + s\theta_0 \quad (10)$$

where $(\Delta r, \theta_d)$ is the position of the disclination with respect to the coordinate origin. For a $s = 1/2$ disclination, the director field is approximately

$$\phi(\theta) = \theta/2 + (\Delta r/2r)\sin(\theta - \theta_d) - \epsilon(3/4)\sin(\theta - \theta_0) + \theta_0/2 \quad (11)$$

The apparent change in the calculated value of ϵ is

$$\Delta\epsilon_{app} = (2/3)(\Delta r/r)\cos(\theta_d - \theta_0) \quad (12)$$

Note that this effect is proportional to $1/r$. The observed structure in Figure 6 also is approximately proportional to $1/r$. Obviously, it is very important to evaluate how much of the observed effect could be due to miscentering. In good quality images, as in Figure 2, the error in miscentering is less than or equal to the lamellar period. The amount of error could contribute at most $1/3$ the observed effect.

Conclusions

The high resolution of electron microscopy together with the lamellar decoration technique of Thomas and Wood enables observation of the disclination core structure in polymer liquid crystals. The near-core structure is analyzed in terms of the apparent bend and splay elastic anisotropy, ϵ_{app}, which is measured as a function of the radial distance from $\pm 1/2$ disclinations both in a rigid and in a flexible-chain TLCP. Results demonstrate that there is an "outer core" approximately 10–20 times the effective molecular length. Frank theory begins to break down at this point, and the deviation from Frank theory varies with molecular rigidity and defect type. The $1/2$ disclination acts only as a source of high distortion, so the deviations are as would be expected on account of molecular rigidity. The rigid material studied splays significantly more at the core. At a radial distance of 0.1 μm, ϵ_{app} is approximately −0.4, yet the asymptotic value, ϵ (at a distance of 1 μm), is approximately 0. The core structure of $-1/2$ disclinations differs from that of the $1/2$ disclination, because splay is avoided. We suggest the presence of an inner core ($r < 3L$), where the lowest MW molecules in the rigid material segregate. In contrast, the flexible material bends more at the core; ϵ_{app} (0.1 μm) ∼ 0.1 and $\epsilon \sim -0.15$. Comparing the outer core sizes of these materials, we suggest approximately one out of every eight spacers may be folded in the flexible polymer. The population of folds does not noticeably increase at the core, indicated by the observation of excess bend in the director field. Because ϵ for both polymers is found to be nearly 0, the effect of neighboring disclinations is found to be fairly well accounted for by an expression which assumes weak anisotropy.

Acknowledgment. We are indebted to Prof. R. W. Lenz, Prof. P. Bhowmik, and Prof. Q. F. Zhou for providing the polymer samples. Financial support was received from the Materials Research Laboratory at the University of Massachusetts, Amherst, the Undergraduate Research Opportunity Program at Massachusetts Institute of Technology through NSF (Polymers Division) Grant DMR 89-07433.

References and Notes

(1) Mermin, N. D. *Rev. Mod. Phys.* **1979**, *51*, 591.
(2) Marrucci, G. *Proc. IX Intl. Congr. Rheol.* **1984**, 441.
(3) Meyer, R. B. *Philos. Mag.* **1973**, *27*, 405.
(4) Cladis, P. E.; Kleman, M. *J. Phys. (Paris)* **1972**, *33*, 591.
(5) Chandrasekhar, S.; Ranganath, G. S. *Adv. Phys.* **1986**, *35*, 507.
(6) Ericksen, J. L. *Liquid Crystals and Ordered Fluids*; Johnson, J. F., Porter, R. S., Eds.; Plenum: New York, 1970; p 181.
(7) Schopohl, N.; Sluckin, T. J. *Phys. Rev. Lett.* **1987**, *59*, 2582.
(8) Mazelet, G.; Kleman, M. *Polymer* **1986**, *27*, 714.
(9) Cladis, P. E.; van Saarloos, W.; Finn, P. L.; Kortan, A. R. *Phys. Rev. Lett.* **1987**, *58*, 222.
(10) Thomas, E. L.; Wood, B. A. *Faraday Discuss. Chem. Soc.* **1985**, *79*, 229.
(11) Hudson, S. D.; Thomas, E. L. *Phys. Rev. Lett.* **1989**, *62*, 1993.
(12) Zhou, Q.-F.; Lenz, R. W. *J. Polym. Sci., Polym. Chem.* **1983**, *21*, 3313.
(13) Lenz, R. W.; Furukawa, F.; Bhowmik, P.; Garay, R. O.; Majnusz, J. *Polymer*, in press.
(14) Krigbaum, W. R.; Tanaka, T. *Macromolecules* **1988**, *21*, 743.
(15) Erman, B.; Flory, P. J.; Hummel, J. P. *Macromolecules* **1980**, *13*, 484.
(16) Hudson, S. D.; Vezie, D. L.; Thomas, E. L. *Makromol. Chem., Rapid Commun.* **1990**, *11*, 657.
(17) Terrel, T. J. *Introduction to Digital Filters*; John Wiley and Sons: New York, 1988.
(18) Caroli, C.; Dubois-Violette, E. *Solid State Commun.* **1969**, *7*, 799.
(19) Nehring, J.; Saupe, A. *J. Chem. Soc., Faraday Trans. 2* **1972**, *68*, 1.
(20) Kaplan, W. *Advanced Mathematics for Engineers*; Addison-Wesley: Reading, MA, 1981; pp 149 and 150.
(21) Meyer, R. B. *Polymer Liquid Crystals*; Ciferri, A., Krigbaum, W. R., Meyer, R. B., Eds.; Academic Press: New York, 1982; pp 133–163.
(22) Odijk, T. *Liq. Cryst.* **1986**, *1*, 553.